

Journal of Materials Chemistry A

Accepted Manuscript



This is an *Accepted Manuscript*, which has been through the Royal Society of Chemistry peer review process and has been accepted for publication.

Accepted Manuscripts are published online shortly after acceptance, before technical editing, formatting and proof reading. Using this free service, authors can make their results available to the community, in citable form, before we publish the edited article. We will replace this *Accepted Manuscript* with the edited and formatted *Advance Article* as soon as it is available.

You can find more information about *Accepted Manuscripts* in the [Information for Authors](#).

Please note that technical editing may introduce minor changes to the text and/or graphics, which may alter content. The journal's standard [Terms & Conditions](#) and the [Ethical guidelines](#) still apply. In no event shall the Royal Society of Chemistry be held responsible for any errors or omissions in this *Accepted Manuscript* or any consequences arising from the use of any information it contains.

The Gas Sensing Properties of Zeolite Modified Zinc Oxide

D.C.Pugh,^a E.J.Newton,^a A.J.T. Naik,^b S.M.V.Hailes^c and I.P. Parkin^{b*}

Cite this: DOI:
10.1039/x0xx00000x

Received 00th January 2012,
Accepted 00th January 2012

DOI: 10.1039/x0xx00000x

www.rsc.org/

The illicit manufacture of drugs in the 21st century presents a danger to first responders, bystanders and the environment, making its detection important. Electronic noses based on metal oxide semiconducting (MOS) sensors present a potential technology to create devices for such purposes. An array of four thick film MOS gas sensors was fabricated, based on zinc oxide inks. Production took place using a commercially available screen printer, a 3 x 3 mm alumina substrate containing interdigitated electrodes and a platinum heater track. ZnO inks were modified using zeolite β , zeolite Y and mordenite admixtures. The sensors were exposed to four gases commonly found in the clandestine laboratory environment; these were nitrogen dioxide, ethanol, acetone and ammonia. Zeolite modification was found to increase the sensitivity of the sensor, compared to unmodified ZnO sensors, all of which showed strong responses to low ppm concentrations of acetone, ammonia and ethanol and to ppb concentrations of nitrogen dioxide. Machine learning techniques were incorporated to test the selectivity of the sensors. A high level of accuracy was achieved in determining the class of gas observed.

Introduction

Metal Oxide Semiconducting (MOS) sensors are a low cost and reliable form of vapour detection. MOS gas sensors operate on the principle that a change in conductivity in the sensing material occurs on contact with a target gas. Their ease of production, high robustness and simple interface electronics make them ideal candidates for commercial detection. They do, however, lack selectivity across a range of analytes¹.

The gas sensing properties of zinc oxide was first demonstrated in 1962 by Seiyama *et.al.*². Zinc oxide has since been found to be a versatile gas sensing material, and has been used in a number of devices, including sensors to detect carbon monoxide^{3,4}, hydrogen^{5,6}, nitrogen oxides^{7,8}, hydrocarbons^{9,10}, alcohols^{11,12,13}, ammonia^{14,15,16} and disulphides¹⁷. The working temperature of ZnO gas sensors is generally quite high, around 400°C-500°C, and selectivity is generally poor¹⁸. As a result of this, preparation methods and doping of ZnO gas sensors to reduce operating temperature and increase selectivity are major research topics^{19,20}.

A good level of selectivity can be obtained by incorporating sensors into an electronic nose. An electronic nose is an array of sensors, used as an analytical instrument, in order to achieve specificity in detecting gases. By using a range of sensor materials, it is possible to achieve a "chemical fingerprint" for a particular gas via a pattern recognition algorithm. MOS gas sensors have been incorporated into a number of electronic noses^{21,22,23,24}, using varying dopants, materials and operating

temperatures to achieve a required fingerprint for a target gas in a wide range of applications^{25,26}.

The data collected by such an instrument can be processed by principal component analysis or classifying techniques such as a support vector machine (SVM). A Support Vector Machine (SVM), proposed by Boser *et.al.*²⁷, is a form of maximum margin classification. Using this technique, a training data set is used to derive an equation that separates classes of data, for example different test gases or concentrations. A basic SVM is a binary classifier: It separates data into two groups. As not all data sets are linearly separable in their standard (input space) form, a function maps the data into higher dimensional space (feature space), and then a linear separating hyperplane is determined. Once the hyperplane for separating the training data has been calculated, the SVM can be used to classify unknown data. The distance between the hyperplane and the nearest data point of each class is calculated to be as large as possible (maximum margin classifier). This is to ensure a greater statistical certainty of classification when separating data.

In order to separate data with more than two classes the algorithm can analyse the data as a series of binary class problems (i.e the ability to determine whether unknown data relates to; gas A/not gas A, gas B/not gas B etc). An SVM will be used in this study to classify multi-class data collected for different target gases.

Four gases that are important target gases for the security industry were tested against three zeolite modified zinc oxide sensors as well as an unmodified ZnO sensor. The four gases are:

Nitrogen Dioxide (NO₂), which is a strong oxidant and toxic atmospheric pollutant. It is frequently found in clandestine laboratories as a side product of the Birch reduction method²⁸. In addition to this, the –NO₂ functional group is a sub structure of many chemicals used in the generation of ammonia for clandestine uses²⁹.

Ethanol (C₂H₅OH), which is a volatile, flammable, colourless liquid, is most commonly used as a solvent and in alcoholic beverages; however, it is also used as a fuel, an intoxicant and in thermometers. It is commonly used in the illicit production of morphine and heroin³⁰.

Ammonia (NH₃) is a strong, colourless, reducing gas and is a key ingredient used in many different methods of production of methamphetamine³¹, as well as potential indicator of homemade explosives³². It is found in a variety of cleaning products and fertilizers; however, it is usually obtained for large-scale clandestine means by theft, or even sale, from the agriculture industry.

Acetone (C₃H₆O) is a flammable, colorless, mobile liquid, and a simple ketone. Acetone is a commonly used solvent for many plastics and synthetic fibers. Acetone is found in the preparation of many illicit substances, including cocaine³³, methamphetamine³⁴ and 3,4-methylenedioxyethylamphetamine (MDMA)³⁵

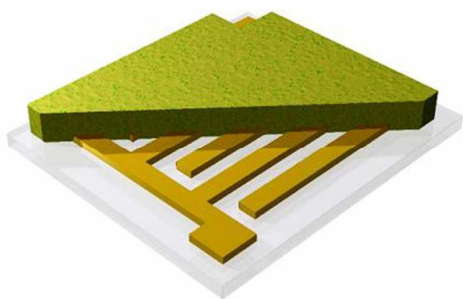


Figure 1 SMO Film on Alumina substrate, showing gold electrodes. The substrate is 3 x 3 mm with 0.15 mm between the interdigitated electrodes. Image courtesy of City Technology Ltd

This work demonstrates the suitability of ZnO and zeolite modified ZnO sensors, as components of an electronic nose, for the detection of volatile compounds of relevance for security applications. It is the first time, to our knowledge, that ZnO and zeolite admixtures have been studied for gas sensing purposes.

Experimental

Zinc oxide was used as supplied by Sigma-Aldrich. Zeolites were used as supplied by Zeolist. H-mordenite, was produced by firing a sample of NH₄-mordenite at 673°C for one hour, as described by Bordiga *et al.*³⁶

All sensors were produced by screen printing metal oxide inks onto 3 x 3 mm alumina substrate tiles, containing laser etched digitated electrodes and an integrated platinum heater track. Inks were produced by mixing a commercially available metal oxide with an organic vehicle (ESL-400, Agmet. Ltd).

Admixtures were created using three types of zeolite: Zeolite Y, Zeolite β and mordenite. All three zeolites have previously been shown to possess gas-separating properties^{37,38,39}. The zeolites used have 3 different structure types (FAU, BEA and MOR respectively). Four different sensors were fabricated, incorporating 30% by mass zeolite material into the ink.

The inks were ground by pestle and mortar to produce a smooth, homogenous suspension. Screen-printing was performed using a DEK1202, ink was printed onto a strip of alumina substrates simultaneously. A total of 5 layers of ink were printed to the substrate. Between applications, the ink was dried under an infra-red lamp for 15 minutes. Following application of all layers, individual sensors were fired for 1 hour at 600°C in an Elite thermal systems BRF15 furnace. The sensors were bonded onto brass pins in a standard polyphenylene sulphide housing using platinum wire (0.0508 mm thickness, supplied by Alfa Aesar) and a MacGregor DC601 parallel gap resistance welder.

Characterisation Techniques

The sensors were characterised by X-ray Diffraction (XRD), Raman Spectroscopy Scanning Electron Microscopy (SEM) and Energy Dispersive X-ray (EDX) spectroscopy, before and after exposure to test gases. XRD diffraction patterns were collected over the 2θ range 10° to 65°, step size 0.02°, on a Bruker GADDS D8 diffractometer using Cu Kα radiation (λ = 0.15418 nm).

Scanning electron micrographs were collected on a Jeol JSM-6301F microscope, in secondary electron imaging mode, using a 5 keV probe voltage. The images were digitally recorded in SemAfore software. EDX analysis was performed using a 20 keV SEM probe coupled with an Oxford Instruments INCA X-Sight system and associated software and confirmed the atomic percentage make up of each sample.

Surface area measurements were made, based on Braunauer-Emmett-Teller (BET) theory, using a Micrometrics ASAP 2420 system. Degassing of samples took place at 150°C. Analysis took place with N₂₍₁₎ at room temperature.

Gas sensing experiments were performed on an in-house testing rig⁴⁰. The rig consists of a 12 port sensing chamber, connected to gas supplies and controlled by four mass flow controllers. A potential divider circuit and an analog to digital converter card allow recording of resistance measurements.

The integrated heater tracks, on the base of the sensor, allowed the working sensor temperatures to be set independently at 350°C, 400°C and 500°C using DC circuitry. Dry compressed air was used as a carrier gas; varying concentrations of test gas were introduced into a fixed flow of 1000 cm³ min⁻¹. Gases were used at proportions between 5%-80% of their supplied concentrations, NO₂ (1 ppm), acetone (10 ppm), ethanol (100 ppm) and ammonia (50 ppm). The sensitivity of sensors was measured as a function of their baseline resistance in compressed air (R_0). For reducing gases, the conductive response (R_0/R) was required, where R is the resistance of the sensor during the test gas pulse. For oxidising gases, the resistive response, the reciprocal of conductive response was used (R/R_0).

Sensors in the test chamber were equilibrated for 20 minutes to establish a baseline resistance; R_0 was calculated as the average resistance during the 2 minutes before the first test gas pulse. Following the initial equilibrium period, five, 600 second, gas pulses took place, with 1200 second air intermissions, to allow sensors to re-establish a baseline resistance R_0 . Gas pulses proceeded with increasing concentration, of 5%, 10%, 20%, 40% and 80% of the cylinder concentration. Tests were repeated in triplicate to ensure repeatability of the sensors. Responses (R_0/R & R/R_0) were used as input to a support vector machine.

Results

X-ray diffraction patterns can be viewed in figure 3 and confirm the chemical make up of the metal oxide and zeolite admixtures. All zinc oxide based materials show a wurzite single-phase structure with high crystallinity, which can be matched with the Joint Committee on Powder Diffraction Standards (JCPDS card no. 36-1451) and literature studies on ZnO⁴¹. With strong peaks at $2\theta = 31.37^\circ$, 34.03° , 35.86° , 47.16° , 56.26° and 62.54° . Additional phases are present in zeolite modified sensors, the diffraction pattern of Zeolite β modified ZnO contains additional peaks at 29.29° , and a doublet at 22.09° and 21.88° , characteristic of the zeolite. The diffraction pattern of Zeolite Y contains additional peaks at 12.43° and a cluster of peaks at around 22° . The diffraction pattern of mordenite modified ZnO contains additional peaks at 13.45° , 22.20° and 25.63° . All are characteristic of their respective zeolites. Additional phases in the modified sensor materials can lead to different gas responses in the sensor. The additional phases are likely due to agglomerated zeolite material, distributed throughout the sensor bulk.

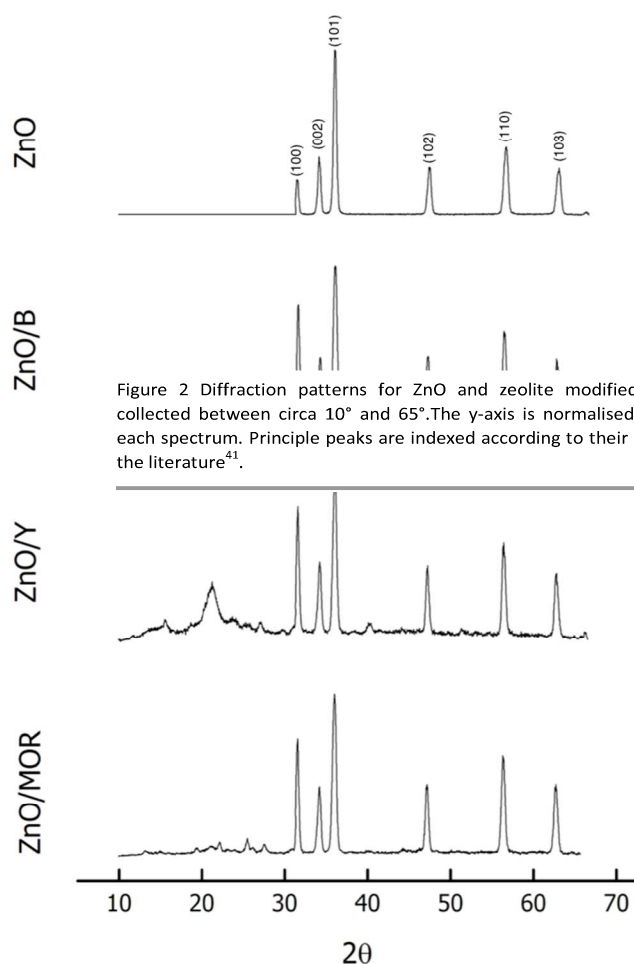


Figure 2 Diffraction patterns for ZnO and zeolite modified ZnO sensors, collected between circa 10° and 65°. The y-axis is normalised and offset for each spectrum. Principle peaks are indexed according to their standards from the literature⁴¹.

SEM micrographs of sensors (in Fig. 4) demonstrate the porous nature of sensor materials and admixtures. The porous nature of unmodified ZnO is demonstrated in Fig 4.A, with smooth circular platelets ranging in size from around 300 nm to 500 nm. The appearance of ZnO and zeolite β admixture (Fig. 4.B), show large “clumps” of ZnO, coated in angular grains of zeolite β that vary in size between 0.1 and 0.4 μm . At higher magnification, it is possible to see high surface area of small grains, around 100 nm in diameter.

Zeolite Y and ZnO admixtures, in fig 4.C, are again porous in nature, exhibiting a cavernous appearance, with grains of around 0.5 μm . At closer magnification, platelet-like grains are visible, approximately 400 nm in diameter.

The cavernous nature of gas sensors is most visible in a Mordenite and ZnO admixture (Fig. 4.D), the material made up of smooth non-uniform grains with an average size of around 600 nm.

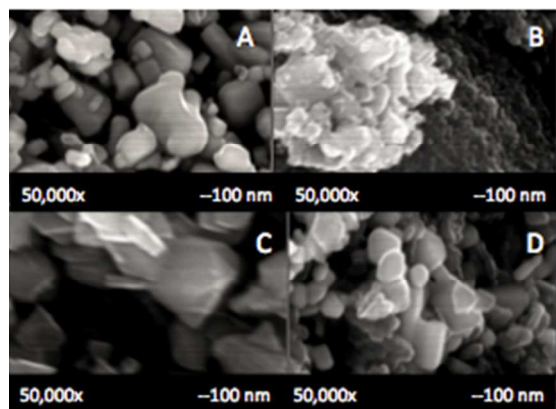


Figure 3 SEM micrographs for each sensor chip. All imaged at 50,000x magnification: (a) ZnO, (b) ZnO/ β , (c) ZnO/Y (d) ZnO/MOR.

The surface area of materials, on their alumina substrate (see table 1), show that admixing with zeolite material increases the surface area of the sensing element by up to 30%, with zeolite β providing the largest increases in surface area, as determined by BET. This increase in surface area can provide increased access to active sites and therefore increase the sensitivity of the gas sensing material.

Table 1 Surface area of ZnO and zeolite modified ZnO sensor chips

Sensor	BET Surface Area (m ² /g)
ZnO	16.8
ZnO/ β	22.1
ZnO/Y	20.1
ZnO/MOR	20.6

Gas Sensing Data

Gas sensing responses are displayed as R_0/R , for reducing gases (acetone, ammonia and ethanol) and R/R_0 , for oxidising gases, where R_0 is the baseline resistance in air, calculated as the average resistance prior to the first gas exposure and R is the resistance in the presence of test gases. An example of the results obtained can be seen in Fig. 4.

Strong resistive responses (an increase in resistance) were recorded upon exposure to NO₂. Sensors were exposed to 0.05, 0.1, 0.2, 0.4 and 0.8 ppm. Zeolite modified sensors showed a much greater degree of sensitivity than unmodified ZnO (up to approximately 100 fold increase) Resistive response was shown to increase with increased concentration. This increase was not linear, but followed an exponential like increase in response at higher concentration.

The gases tested showed varying responses to temperature dependent on the gas present. Under NO₂ exposure, resistive response decreased, with increasing temperature.

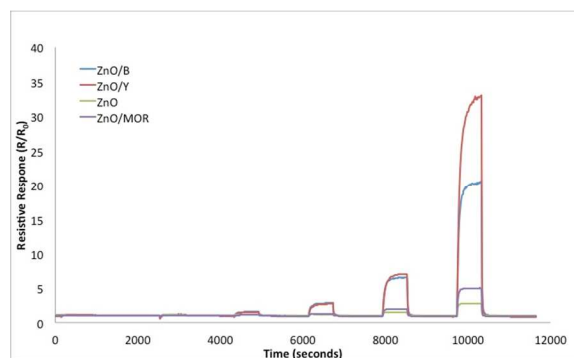


Figure 4 Plot of ZnO and zeolite modified ZnO sensors to 0.05, 0.1, 0.2, 0.4 and 0.8 ppm NO₂ at 500°C

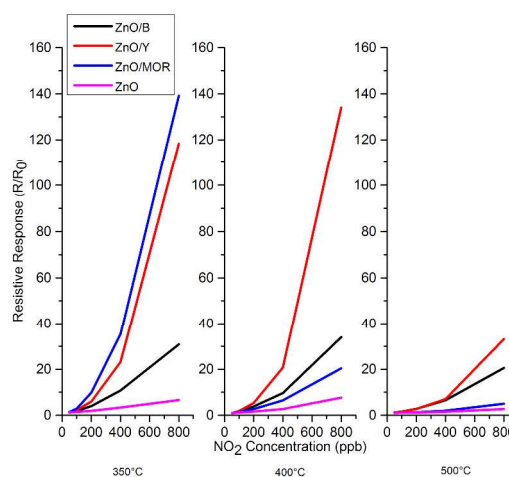


Figure 5 Sensor responses to NO₂ at concentrations between 0.05 and 0.8 ppm, at 350, 400 and 500°C in dry air for a 600 s exposure.

Sensor exposure to 5, 10, 20, 40 and 80 ppm ethanol produced strong conductive responses (decreases in resistance, shown as R_0/R). At 500°C admixture sensors offered large enhancements in sensitivity, in comparison to unmodified zinc oxide. Ethanol exposure gave a maximum conductive response at 400°C, ZnO showing the largest magnitude of response, at 400°C, from $R/R_0 = 6.59$, in unmodified zinc oxide, to $R/R_0 = 143$, in a zinc oxide and mordenite admixture. A decrease in resistance is observed during exposure to an ethanol gas pulse; this is because ethanol, as a reducing gas, has a different mechanism of action to NO₂, resulting in the introduction of electrons to the sensing element, therefore increasing conductivity and lowering resistance, due to the decrease in size of the electron depletion region in the material⁴².

The magnitude of response increased with gas concentration. This is because more ethanol was available for redox reactions at the sensor surface when concentration of test gas in air was higher. The maximum responses of sensors, under exposure to ethanol, are shown in figure 6. All sensors show maximum conductive responses at 400°C, with the exception of ZnO and mordenite admixture sensor, which shows a maximum response

at 500°C. An unmodified zinc oxide thick film sensor, at 400°C, shows a large increase in conductive response.

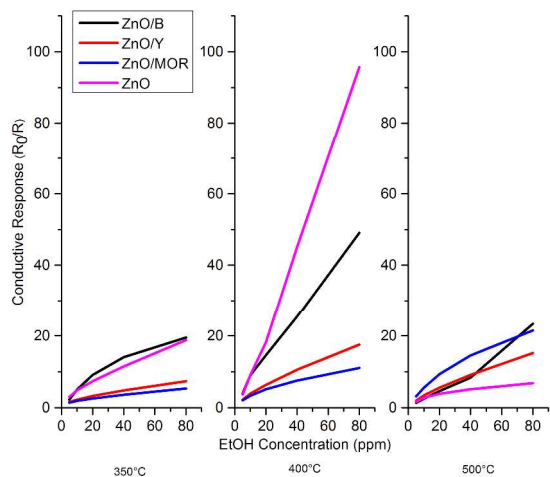


Figure 6 Sensor responses to EtOH at concentrations between 5 and 80 ppm, at 350°C, 400°C and 500°C in dry air for a 600 s exposure.

The exposure of sensors to 0.5, 1, 2, 4 and 8 ppm acetone also produced strong conductive responses. At 500°C, zeolite modified sensors offered reduced sensitivity, over unmodified Zinc oxide. However at lower operating temperatures, the magnitude in sensitivity of zeolite modified sensors increases, presenting larger magnitudes than unmodified ZnO. Acetone exposure gave a maximum conductive response at 400°C in Zeolite β modified ZnO. Unmodified ZnO showed the largest magnitude of response, at 500°C.

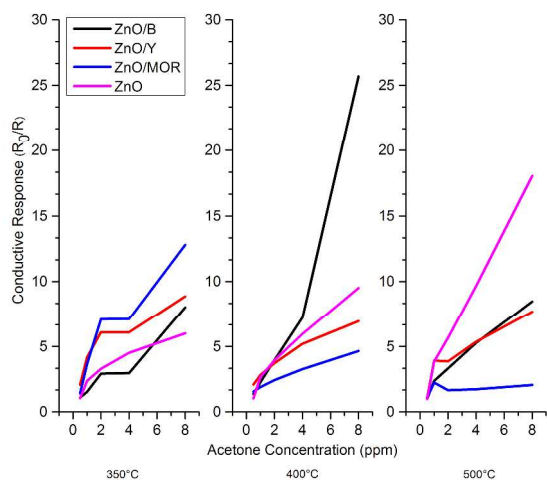


Figure 7 Sensor responses to acetone at concentrations between 0.5 and 8 ppm, at 350°C, 400°C and 500°C in dry air for a 600 s exposure.

Sensors were also exposed, to 2.5, 5, 10, 20 and 40 ppm of ammonia. This exposure produced strong conductive responses; with up to an 8 fold decrease in resistance. The magnitude of maximum response decreased with increasing temperature.

Ammonia also underwent multiple reactions at the sensor surface, causing an initially strong conductive response (a decrease in resistance). Response then decreased for the remainder of the gas pulse (see Fig.8). This shows that after a brief period, one of the multiple reactions taking place at the surface dominates, giving a single response.

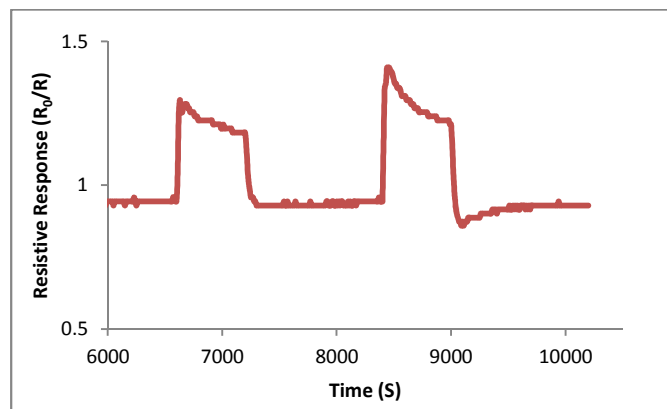


Figure 8 Conductive response of zeolite Y doped ZnO upon exposure to 20 and 40 ppm ammonia at 400°C, demonstrating the unusual peak shape observed under acetone exposure, comprised of an initial peak, followed by a decline in magnitude for the remainder of the exposure time.

All sensors showed a larger magnitude of conductive response, at higher concentrations, due to the increased availability of ammonia in the environment to react at the sensor surface.

Figure 8 shows a plot the maximum conductive response of ammonia against concentration and shows that an enhanced conductive response, at higher temperatures.

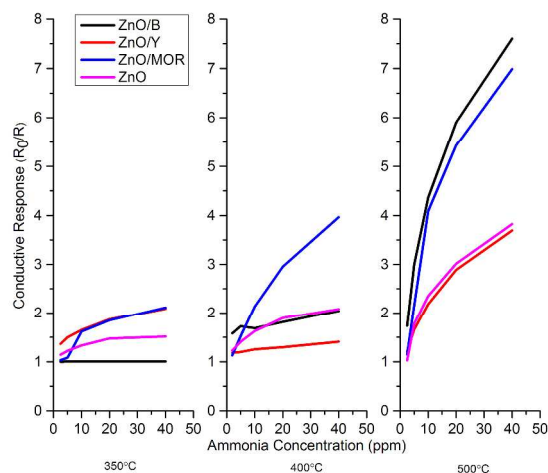


Figure 9 Sensor responses to ammonia at concentrations between 2.5 and 40 ppm, at 350, 400 and 500°C in dry air for a 600 s exposure.

A supervised learning technique was applied to a subset of the data collected. The tool used was Sequential Minimal Optimisation (SMO), designed by Platt⁴³. This applied a “one

against one technique”, to separate multiple classes, as an efficient implementation of an SVM⁴⁴. Analysis was performed using the data-mining package WEKA⁴⁵.

The data set used in classification contained details of the maximum response found in each gas pulse, along with the first 5 conductive and resistive response values, representing the change in resistivity in the first 50 seconds of each gas pulse. In addition to this, information on the temperature and type of sensor used were incorporated into the dataset.

This provided an excellent classification of gas type, with 92% accuracy. A confusion matrix of the data is shown in table 2.

	NO ₂	NH ₃	EtOH	Acetone
NO ₂	59	0	0	1
NH ₃	0	57	3	0
EtOH	0	10	50	0
Acetone	1	1	3	55

Table 2 Confusion matrix for the 10 fold cross validation, using optimised cost function. The class is defined vertically and the output classification is shown horizontally.

Of the four gases tested, NO₂ was the most easily recognisable, due to the difference in its response type (resistive, as opposed to conductive response) to the three other gases, which exhibited conductive responses. There was some confusion in classifying between ethanol and ammonia, due to their similar conductive responses. It should be possible to increase the success of classification by introducing more sensors into the array, with additional metal oxides and transformational elements such as filters and separation units⁴⁶.

The results of unmodified zinc oxide sensors exposure were consistent with literature sensitivities for each of the four test gases; acetone⁴⁷, ammonia⁴⁸, ethanol⁴⁹ and nitrogen dioxide⁵⁰. Exposure to all test gases resulted in an increased sensitivity in zeolite modified sensors. This is likely due to the open microstructure of sensor materials, as well as the catalytic activity of the zeolites, in the bulk sensor material. It has been hypothesised that zeolites, being insulating materials, restrict the percolation of electrons through the material, increasing resistance and aiding in resistive response of the material, as shown on exposure to NO₂. These actions are different to sensors where zeolite layers are applied as overlayers, where the zeolite acts as a filter to filter out molecules that are too large for the pore size as well as catalytic activity taking place within the zeolite itself.

At different temperatures, sensors gave different magnitudes of response at different temperatures, There are a number of reasons for this; adsorption and desorption at the sensor surface are temperature activated, the physical properties of the material, such as charge carrier concentration, Debye length and work function. The rate of reaction for the oxidation/

reduction of a specific test gas is dependant on the gas. A peak temperature for maximum sensitivity, below this maximum the rate of reaction is too slow to give the maximum sensitivity, whereas if the temperature is too high, the redox reaction proceeds so rapidly that the concentration of the test gas becomes diffusion limited and the concentration seen by the sensor approaches zero⁵¹. At such temperatures, redox reactions can take place at the sensor surface without producing a noticeable electric charge on the metal oxide material.

Results of the gas tests, repeated in triplicate showed a good level of reproducibility, with all results with less than 2% variation in identical tests.

Classification of the sensors, with XRD, SEM and EDX after exposure to the gases showed no change in the microstructure of the material, indicating the potential for good long term stability of the sensor material. While many different types of sensor are available, MOS sensors present a number of advantages over other sensor instrumentation such as optical and electrochemical sensors. MOS sensors are not affected by stray light, and can give an indication as to the concentration of a gas, unlike optical sensors⁵².

Importantly, MOS sensors, at a cost of around \$14 a sensor⁵³, are much cheaper to produce than electrochemical⁵⁴, gravimetric⁵⁵, and ionisation sensors⁵⁶.

Conclusions

A sensor array of four sensors, incorporating three different zeolites was manufactured. This is the first time zeolites have been incorporated into ZnO, forming zeolite admixture sensors. Admixed sensors showed a large increase in sensitivity to NO₂ (from R/R₀ = 6 with unmodified ZnO to R/R₀ = 142, for ZnO doped with mordenite) and at higher temperatures, to ethanol (from R₀/R = 7 to R₀/R = 23).

Post exposure characterisation of the sensor materials found that neither heating of the sensors nor exposure to any of the test gases used, caused any structural change to the materials, indicating that unmodified ZnO and zeolite doped ZnO would present strong repeatability and reproducibility over a longer time period.

Zeolite modified zinc oxide sensors show a larger magnitude of response to similar concentrations of NO₂ than WO₃ and In₂O₃ sensors²⁵, a larger response to ethanol than SnO₂ sensors⁵⁷ and a larger response to acetone than Fe₂O₃ gas sensors⁵⁸.

All results were subjected to machine learning techniques and achieved good accuracy (~92%) in determining the class of gas to which sensors were exposed. The ease of production of sensor materials, combined with the low cost of the electronics, mean that the sensing array shows good promise for the

development of an electronic nose based on semiconducting metal oxide technology.

Acknowledgements

Dr Steve Firth, Jessica Ellis, Kevin Reeves and Martin Vickers are thanked for their help with the instrumentation. This work was carried out under EPSRC Grant no: EP/G037264/1 as part of UCL's Security Science Doctoral Training Centre.

Notes and references

^aDept. of Security and Crime Science, University College London, 35 Tavistock Sq., London, WC1H 9EZ, UK. E-mail: d.pugh.12@ucl.ac.uk

^bDept. of Chemistry, University College London, 20 Gordon St., London, WC1H 0AJ, UK.

^cDept. of Computer Science, University College London, Gower St., London, WC1E 6BT, UK

- 1D.P. Mann, T. Paraskeva, K. F. E. Pratt, I. P. Parkin, and D. E. Williams. *Measurement Science and Technology*, 2005, **16**, 1193.
- 2S. Tetsuro, A. Kato, K. Fujiishi, and M Nagatani. *Analytical Chemistry*, 1962, **34**, 1502.
- 3 J. H. Yu and G. M. Choi, *Sensors and Actuators B*, 1999, **61**, 59.
- 4 B. Bott, T. A. Jones, and B. Mann, *Sensors and Actuators*, 1984, **5**, 65.
- 5 M. Egashira, N. Kanehara, Y. Shimizu, and H. Iwanaga, *Sensors and Actuators*, 1989, **18**, 349.
- 6S. Saito, M. Miyayama, K. Koumoto, and H. Yanagida, *Journal of the American Ceramic Society*, 1985, **68**, 40.
- 7 R. Lambrich, W. Hagen, and J. Logois, *Analytical Chemistry Symposia Series*, 1983 **17**, 73.
- 8 P. Romppainen, V. Lantto, and S. Leppavuori, *Sensors and Actuators B*, 1990, **1**, 73.
- 9 C. N. R. Rao, A. R. Raju, and K. Vijayamohan, Gas-Sensor Materials, in New Materials (S. K. Joshi, T. Tsuruta, C. N. R. Rao, and S. Nagakura, Eds., Narosa, New Delhi, 1992, and the references therein).
- 10 G. Williams and G. S.V. Coles, *Sensors and Actuators B*, 1999, **57**, 108.
- 11 B. P. J. d. L. Costello, R. J. Ewen, N. M. Ratcliffe, and P. S. Sivanand, *Sensors and Actuators B*, 2003, **92**, 159.
- 12 A. R. Raju and C. N. R. Rao, *Sensors and Actuators B*, 1991, **3**, 305–310.
- 13 B.P. de Lacy Costello, R.J. Ewen, N. Guernion, N.M. Ratcliffe, *Sensors and Actuators B*, 2002, **87**, 207.
- 14 M. Egashira, Y. Shimizu, and Y. Takao, *Sensors and Actuators B*, 1990, **1**, 108.
- 15 H. Nanto, T. Minami, and S. Takata, *Journal of Applied Physics*, 1986, **60**, 482.
- 16 M.S. Wagh, G.H. Jain, D.R. Patil, S.A. Patil, and L.A Patil, *Sensors and Actuators B*, 2006, **115**, 128.
- 17 B. P. J. d. L. Costello, R. J. Ewen, P. R. H. Jones, N. M. Ratcliffe, and R. K. M. Wat, *Sensors and Actuators B*, 1991, **61**, 199.
- 18 S.R. Morrison. *Sensors and Actuators*, 1987, **12**, 425.
- 19 X. Lou, *Journal of Sensor and Transistor Technology*, 1991, **3**, 1.
- 20 Cheng, X. L., H. Zhao, L. H. Huo, S. Gao, and J. G. Zhao. *Sensors and Actuators B*, 2004, **102**, 2, 248.
- 21 S.S Chowdhury, B. Tudu, R. Bandyopadhyay, and N. Bhattacharyya. In *Industrial and Information Systems, 2008. ICIIS 2008. IEEE Region 10 and the Third international Conference on*, pp. 1-5. IEEE, 2008.
- 22 M. Ghasemi-Varnamkhasi, S.S. Mohtasebi, M.L. Rodriguez-Mendez, J. Lozano, S. H. Razavi, and H. Ahmadi, *Trends in Food Science & Technology* 22, 2011, **4**, 165.
- 23 M. Falasconi, I. Concina, E. Gobbi, V. Sberveglieri, A. Pulvirenti, and G. Sberveglieri. *International Journal of Electrochemistry* 2012 (2012).
- 24 A.D. Wilson, *Sensors*, 2013, **13**, 2295.
- 25 W.J. Peveler, R. Binions, S.M.V. Hailes, and I.P. Parkin. *Journal of Materials Chemistry A*, 2013, **7**, 2613.
- 26 K. Arshak, E. Moore, G.M. Lyons, J. Harris, & S. Clifford, *Sensor Review*, 2004, **24**, 181.
- 27 B. E. Boser, I. M. Guyon, and V. Vapnik, "A training algorithm for optimum margin classifiers." in *Proceedings of the fifth annual workshop on computational learning theory*. ACM, 1992. 144
- 28 J.L. Hughart, *Arhiv za Higijenu Rada I Toksikologiju/Archives of Industrial Hygiene and Toxicology*, 2000, **51**, 305.
- 29 L.A. Knops, D.M. Northrop, and E.C. Person. " *Journal of forensic sciences*, 2006, **51**, 82.
- 30 K.R. Bedford, S.L. Nolan, R. Onrust, & J.D. Siegers, *Forensic Science International*, 1987, **34**, 197-204.

- 31 J.W. Martyny, S.L. Arbuckle, C.S. McCammon Jr, E.J. Esswein, N. Erb, and M. Van Dyke. *Journal of Chemical Health and Safety*, 2007, **14**, 40.
- 32 K. Wells, and D. A. Bradley. *Applied Radiation and Isotopes*, 2012, **70**, 1729.
- 33 W.H. Soine, *NIDA Research Monograph*, 1989, **95**, 44-50.
- 34 H.F. Skinner. *Forensic science international*, 1990, **48**, 123.
- 35 R.J. Renton, J. S. Cowie, and M. C. H. Oon. *Forensic science international* 1993, **60**, 189.
- 36 S. Bordiga, C. Lamberti, F. Geobaldo, A. Zecchina, G. Turnes Palomino, and C. Otero Areán. *Langmuir*, 1995, **11**, 527.
- 37 O. Hugon, M. Sauvan, P. Benech, C Pijolat, and F. Lefebvre. *Sensors and Actuators B*, 2000, **67**, 235.
- 38 J.A. Martens, J. Perez-Pariente and P.A. Jacobs, in: *Chemical Reactions in Organic and Inorganic Constrained Systems*, NATO ASI Ser. C. 165 (1986) 115.
- 39 Coronas, J., and J. Santamaria. *Chemical engineering science*, 2004, **59**, 4879.
- 40 S. C. Naisbitt, K. F. E. Pratt, D. E. Williams and I. P. Parkin, *Sensors and Actuators, B*, 2006, **114**, 969.
- 41 J.L. Van Heerden, and R. Swanepoel. *Thin Solid Films*, 1997, **299**, 72.
- 42 K. Wetchakun, T. Samerjai, N. Tamaekong, C. Liewhiran, C. Siritwong, V. Kruefu, A. Wisitsoraat, A. Tuantranont, and S. Phanichphant. *Sensors and Actuators B: Chemical* 2011, **160**, 580.
- 43 Platt, "Sequential minimal optimization: A fast algorithm for training support vector machines." (1998).
- 44 C.-W. Hsu and C.-J. Lin, *Neural Networks*, IEEE Transactions on, 2002, **13**, 415.
- 45 WEKA 3- Data Mining with Open Source Machine Learning Software <http://www.cs.waikato.ac.nz/ml/weka/>
- 46 F. Röck, N. Barsan, and U Weimar. *Chemical Reviews*, 2008, **108**, 705.
- 47 H. Nanto, T. Minami, S. Takata, *Journal of Applied Physics*. 1986, **60**, 482.
- 48 A. Patil, C. Dighavkar, R. Borse, S. Patil, and R. Khadayate, *Journal of Electron Devices*, 2012, **15**, 1274.
- 49 Kalyan Chakravarthi, M., and B. Bharath. In *Mechatronics and its Applications (ISMA), 2012 8th International Symposium*. IEEE, 2012, 1.
- 50 M. Yongki, H. Tuller, S. Palzer, J. Wöllenstein, and H. Böttner. *Sensors and Actuators B*, 2003, **1**, 435.
- 51 N. Yamazoe, G. Sakai and K. Shinamoe. *Catalysis surveys from Asia*, 2003, **7**, 63.
- 52 S. Satyanarayana, Surface stress and capacitive MEMS sensor arrays for chemical and biological sensing, Ph.D. thesis, University of California, Berkeley, 2005.
- 53 Figaro, TGS826 TGS2444 TGS2620, Osaka, Japan
- 54 BW Technologies, GasAlert Extreme, Calgary, Alberta, Canada
- 55 Electronic Sensor Technology, zNose 4200, Newbury Park, CA, USA
- 56 RAE Systems, AreaRAE, MiniRAE 2000, MiniRAE 3000, ppbRAE 3000, ppbRAE Plus, RAEGuard PID, San Jose, CA, USA. [82]
- 57 T. Jinkawa, G. Sakai, J. Tamaki, N. Miura, and N. Yamazoe. *Journal of Molecular Catalysis A: Chemical*, 2000, **155**, 193.
- 58 S. V. Ryabtsev, A. V. Shaposhnick, A. N. Lukin, and E. P. Domashevskaya, *Sensors and Actuators*, 1999, **B59**, 26.